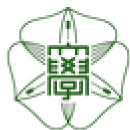
HOKKAIDO UNIVERSITY

Title	Reduced thermal resistance in AlGaN/GaN multi-mesa-channel high electron mobility transistors
Author(s)	Asubar, Joel T.; Yatabe, Zenji; Hashizume, Tamotsu
Citation	Applied Physics Letters, 105(5), 53510 https://doi.org/10.1063/1.4892538
Issue Date	2014-08-04
Doc URL	http://hdl.handle.net/2115/57547
Rights	Copyright 2014 American Institute of Physics. This article may be downloaded for personal use only. Any other use requires prior permission of the author and the American Institute of Physics. The following article appeared in Applied Physics Letters 105, 053510 (2014); doi: 10.1063/1.4892538 and may be found at http://dx.doi.org/10.1063/1.4892538.
Type	article
File Information	1.4892538.pdf

Instructions for use

Hokkaido University Collection of Scholarly and Academic Papers : HUSCAP

AIP Applied Physics Letters

Reduced thermal resistance in AlGaN/GaN multi-mesa-channel high electron mobility transistors

Joel T. Asubar, Zenji Yatabe, and Tamotsu Hashizume

Citation: Applied Physics Letters **105**, 053510 (2014); doi: 10.1063/1.4892538
View online: http://dx.doi.org/10.1063/1.4892538
View Table of Contents: http://scitation.aip.org/content/aip/journal/apl/105/5?ver=pdfcov
Published by the AIP Publishing

Articles you may be interested in
Effect of proton irradiation on thermal resistance and breakdown voltage of InAlN/GaN high electron mobility transistors
J. Vac. Sci. Technol. B **32**, 051203 (2014); 10.1116/1.4891629

Probing channel temperature profiles in AlxGa1−xN/GaN high electron mobility transistors on 200mm diameter Si(111) by optical spectroscopy
Appl. Phys. Lett. **105**, 073504 (2014); 10.1063/1.4893603

AlGaN/GaN high-electron mobility transistors with low thermal resistance grown on single-crystal diamond (111) substrates by metalorganic vapor-phase epitaxy
Appl. Phys. Lett. **98**, 162112 (2011); 10.1063/1.3574531

Finite-element simulations of the effect of device design on channel temperature for AlGaN/GaN high electron mobility transistors
J. Vac. Sci. Technol. B **29**, 020603 (2011); 10.1116/1.3567183

Surface strain and its impact on the electrical resistivity of GaN channel in AlGaN/GaN high electron mobility transistor
Appl. Phys. Lett. **93**, 222106 (2008); 10.1063/1.3040315

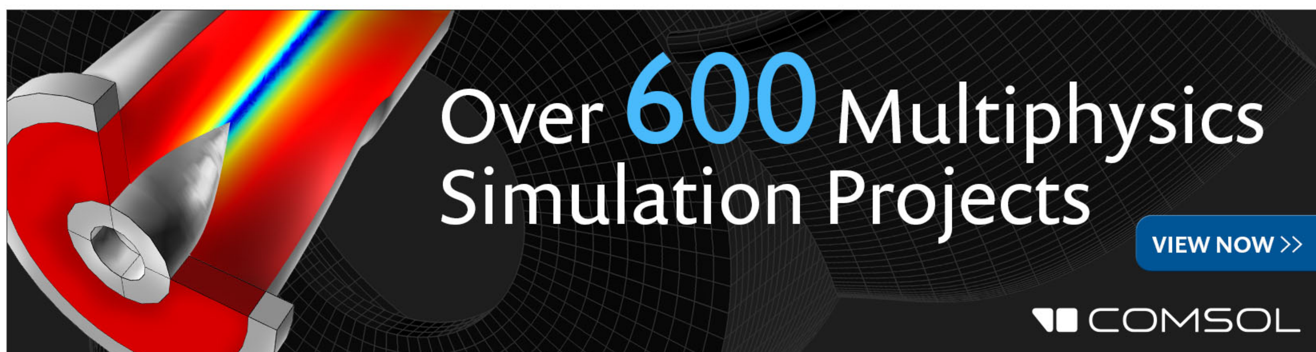

This article is copyrighted as indicated in the article. Reuse of AIP content is subject to the terms at: http://scitation.aip.org/termsconditions. Downloaded to IP: 133.87.166.132 On: Tue, 16 Dec 2014 06:13:52

Reduced thermal resistance in AlGaN/GaN multi-mesa-channel high electron mobility transistors

Joel T. Asubar,[1,2,a)] Zenji Yatabe,[1,2] and Tamotsu Hashizume[1,2]
[1]*Research Center for Integrated Quantum Electronics (RCIQE) and Graduate School of Information Science and Technology, Hokkaido University, Sapporo, Japan*
[2]*Japan Science and Technology Agency (JST), CREST, 102-0075 Tokyo, Japan*

(Received 26 May 2014; accepted 26 July 2014; published online 7 August 2014)

Dramatic reduction of thermal resistance was achieved in AlGaN/GaN Multi-Mesa-Channel (MMC) high electron mobility transistors (HEMTs) on sapphire substrates. Compared with the conventional planar device, the MMC HEMT exhibits much less negative slope of the I_D-V_{DS} curves at high V_{DS} regime, indicating less self-heating. Using a method proposed by Menozzi and co-workers, we obtained a thermal resistance of 4.8 K-mm/W at ambient temperature of ∼350 K and power dissipation of ∼9 W/mm. This value compares well to 4.1 K-mm/W, which is the thermal resistance of AlGaN/GaN HEMTs on expensive single crystal diamond substrates and the lowest reported value in literature. © *2014 AIP Publishing LLC*. [http://dx.doi.org/10.1063/1.4892538]

Gallium Nitride (GaN) is considered as one of the leading material candidates for realizing next-generation electronics devices capable of handling unprecedented power levels.[1] However, due to thermal limitation of conventionally used substrate materials, usable power densities are limited to 5–8 W/mm.[2] At high power dissipation, the problem of self-heating, which is usually manifested as a negative slope of the I_D-V_{DS} curves at high V_{DS} regime, becomes critical, especially on devices fabricated on the common but thermally resistive sapphire substrates.[3–5] Self-heating leads to increased channel temperature which not only reduces the electron mobility and saturation velocity[6] but also decreases the median time to failure of power devices.[7] Moreover, self-heating may lead to a thermally-induced breakdown at voltage levels lower than the theoretically predicted value.[8] Since it is widely believed that the generated Joule heat mainly dissipates through the substrate, the obvious solution is to use low thermal resistivity but expensive substrates such as SiC,[9] and GaN.[10] Recently, Hirama and co-workers have reported a thermal resistance record value of 4.1 K-mm/W for an AlGaN/GaN HEMT fabricated on single-crystal diamond.[11] Riedel *et al.* were able to further reduce the thermal resistance of AlGaN/GaN HEMTs on SiC using a hot-wall metal organic chemical vapor deposition (MOCVD) grown aluminum nitride (AlN) nucleation layer, which lowers the thermal-boundary resistance between GaN and SiC.[12] Self-heating had also been addressed using heat spreading layers such as thick AlN surface passivation films.[13] Using flexible graphene quilts precisely transferred over the drain contacts, Yan *et al.* demonstrated lowering the hotspot temperature by as much as 20 °C.[14] Various flip-chip bonding techniques have also been shown to be effective in improving thermal performance of AlGaN/GaN HEMTs.[15,16] In this Letter, we report dramatic reduction of thermal resistance in AlGaN/GaN MMC HEMTs fabricated on sapphire substrates. Our structure-based approach offers an alternative avenue in mitigating self-heating problems in AlGaN/GaN HEMTs. Using a technique proposed by Menozzi and co-workers,[17] we extracted the thermal resistance of the MMC and compared it with that of the conventional planar device fabricated on the same chip.

The AlGaN/GaN MMC HEMT is schematically illustrated in Fig. 1. The parallel nano-channels structure facilitates the modulation of the two-dimensional electron gas (2DEG) vertically from the top and laterally through the sidewalls, improving gate controllability and shifting the threshold voltage V_{TH} towards the normally-OFF voltage direction.[18] Moreover, due to the resulting nano-channel high impedance, the MMC HEMT is less sensitive to changes in the access region; may they be due to trapping or changes in the physical dimension like gate-drain (G-D) spacing L_{GD}, providing better current stability and breakdown voltage design flexibility compared with the planar HEMT.[18–20] Very recently, several groups have reported improved performance from nitride-based devices with very similar structure. Lee *et al.* have demonstrated nanowire channel InAlN/GaN HEMTs with high linearity of both transconductance g_m and cut-off frequency f_t.[21] Simin *et al.* have demonstrated in their perforated-channel AlGaN/GaN HEMTs significant reduction

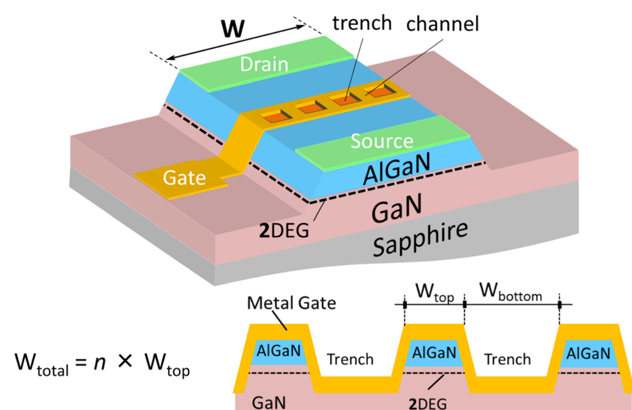

FIG. 1. Schematic illustration of the AlGaN/GaN MMC HEMT. The total effective gate width W_{total} is equal to $n \times W_{top}$, where n is the number of mesa-channels and W_{top} is the width of each mesa-channel.

a)E-mail: joel@rciqe.hokudai.ac.jp

 © 2014 AIP Publishing LLC

This article is copyrighted as indicated in the article. Reuse of AIP content is subject to the terms at: http://scitation.aip.org/termsconditions. Downloaded to IP: 133.87.166.132 On: Tue, 16 Dec 2014 06:13:52

of on-resistance-gate capacitance ($R_{ON}C_G$) product, significantly improving the transistor operation in power switches and amplifiers.[22]

The $Al_{0.23}Ga_{0.77}N$/GaN heterostructure used in the present study was grown by MOCVD technique on (0001) sapphire substrates. The thickness of the AlGaN barrier layer is 25 nm. The typical values of 2DEG sheet density and mobility at room temperature (RT) are $9.0 \times 10^{12}\,\mathrm{cm}^{-2}$ and $1330\,\mathrm{cm}^2/\mathrm{Vs}$, respectively. The fabrication process is similar to that discussed in Ref. 20. To extract the thermal resistance (R_{TH}) of the devices, we applied the technique proposed by Menozzi and co-workers,[17] which only requires measurement of DC I_D-V_{DS} curves at different ambient temperature T_A. Thus, with the exception of an accurate and stable temperature controller, this technique requires very standard and relatively inexpensive experimental set-up. This method assumes a linear dependence of saturation drain current I_D on channel temperature T_C once the linear dependence of I_D on ambient temperature T_A is established. In principle, it is possible to limit the temperature range so that I_D varies with T_A linearly.[17,23] Indeed, the linear relationship of AlGaN/GaN HEMTs I_D and T_A has been verified experimentally by several research groups.[14,24,25] Aside from choosing a suitably narrow intervals of T_A and power dissipation P_D, wherein the I_D dependence on T_A can be linearized with accuracy and R_{TH} can be considered constant, no other simplifying assumption is necessary.[17] The physical basis of this method is discussed below.

In analogy to electrical resistance, the thermal resistance R_{TH} (Ref. 17) can be given by

$$R_{TH} = \frac{\Delta T}{P_D} = \frac{T_C - T_A}{V_{DS} \times I_D} = \frac{T_{C0} - T_{A0}}{V_{DS} \times I_{D0}}. \quad (1)$$

Here, ΔT is the difference between the device channel temperature T_C and ambient temperature T_A, P_D is the device power dissipation which is the product of a fixed drain to source voltage V_{DS} and saturation drain current I_D. At a reference ambient temperature T_{A0}, at the same V_{DS}, the corresponding values of channel temperature, and drain current are T_{C0} and I_{D0}, respectively. Assuming linear relationship of I_D and temperature, then

$$I_D = I_{D0} + h(T_A - T_{A0}) \quad (2)$$

and

$$I_D = I_{D0} + h'(T_C - T_{C0}), \quad (3)$$

where, h and h' are proportionality constants. Substituting Eqs. (2) and (3) to (1) and simplifying, it easy to obtain the following relationship:

$$\frac{1}{h} = \frac{1}{h'} - R_{TH}V_{DS}. \quad (4)$$

Thus, R_{TH} is the slope of the variation of $1/h$ with V_{DS}. Figure 2 summarizes further in a flowchart the R_{TH} extraction method.

Figures 3(a), inset of 3(b), and 3(b) show the T_A dependence of I_D-V_{DS} curves, V_{DS} dependence of I_D-T_A plots, and the $1/h$-V_{DS} plot, respectively, of the planar device while

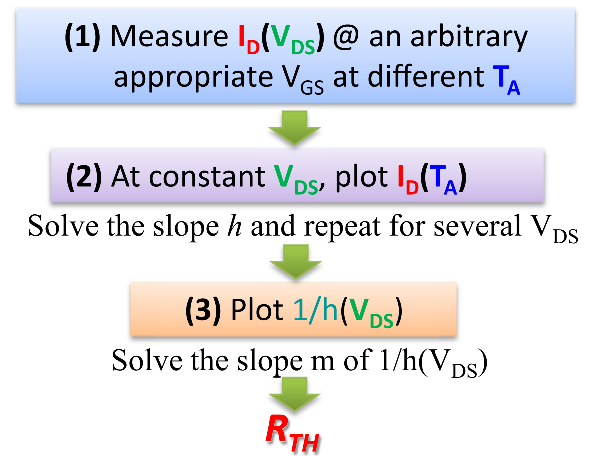

FIG. 2. Simplified flowchart of the thermal resistance R_{TH} extraction from the I_D-V_{DS}-T_A plots proposed by Menozzi *et al.*[17]

Figure 4 shows the same set of data for the MMC device having same levels of raw I_D. The DC I_D-V_{DS} characteristics were measured using an Agilent B1500A semiconductor device parameter analyzer while the ambient-chuck temperature was precisely controlled by a Vector Semiconductor THC-151 thermocontroller. A starting temperature of 42 °C was chosen because it is the lowest temperature closest to RT that can be controlled in the present experimental setup. Both devices investigated have gate lengths L_G of 1 μm, gate-drain spacing L_{GD} of 10 μm, and gate-source spacing

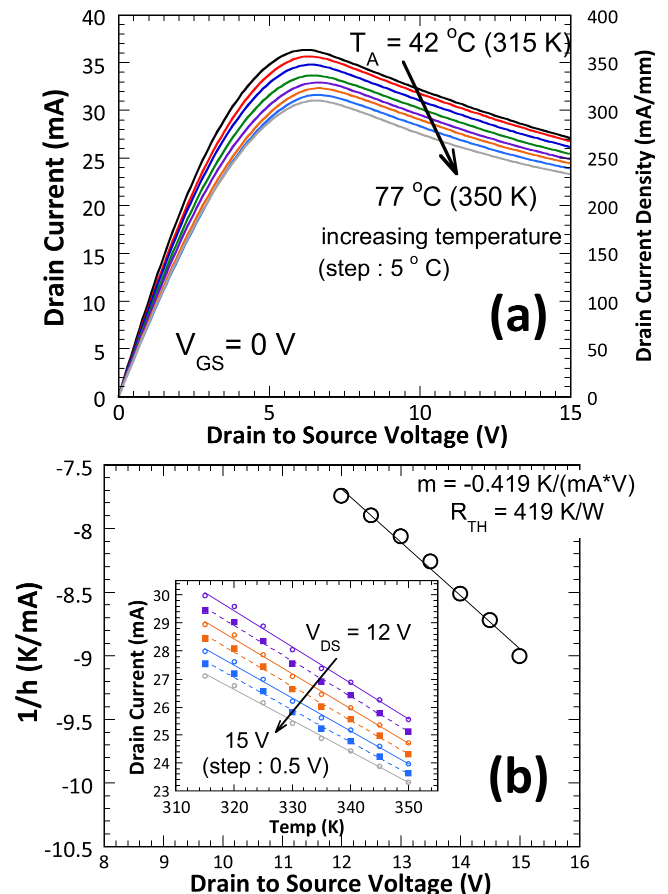

FIG. 3. Planar device with W of 100 μm (a) T_A dependence of I_D-V_{DS} curves, ((b), inset) V_{DS} dependence of I_D-T_A plots, (b) $1/h - V_{DS}$ plot.

This article is copyrighted as indicated in the article. Reuse of AIP content is subject to the terms at: http://scitation.aip.org/termsconditions. Downloaded to IP: 133.87.166.132 On: Tue, 16 Dec 2014 06:13:52

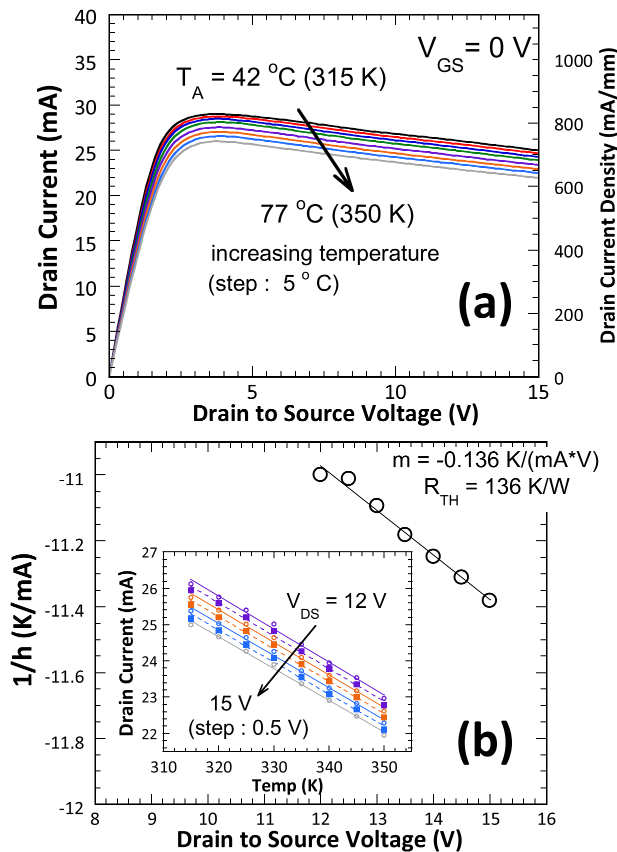

FIG. 4. MMC device with W_{top} of 70 nm and W_{total} of 35 μm (a) T_A dependence of I_D-V_{DS} curves, ((b), inset) V_{DS} dependence of I_D-T_A plots, (b) $1/h - V_{DS}$ plot.

L_{GS} of 2 μm. The planar device has a gate width W of 100 μm. Scanning electron microscopy investigations revealed that the MMC device has a W_{top} of ~70 nm. Since there are 500 periods of mesa-trench structures within the gate electrode width of 200 μm, the effective total gate width W_{total} is 35 μm for the MMC device. The threshold voltage V_{TH} values are -1.8 V and -3.7 V for the MMC and planar devices, respectively. The MMC device showed significantly less knee voltage V_{knee} consistent with our previous reports.[18–20] Even though its effective gate width W_{total} is just almost a third of that of the planar device, the MMC device exhibited almost the same levels of raw I_D. At T_A of 42 °C, $V_{GS} = 0$ V, and $V_{DS} = 15$ V, the MMC and planar devices have raw I_D of ~25 mA and ~27 mA, respectively. Solving for the drain current density I_{DS_den} (raw I_D divided by the effective gate width W_{total}), the above values translate to 714 mA/mm and 270 mA/mm, respectively for the MMC and planar devices. As can be seen in Fig. 3(a), the planar device suffers from severe self-heating as indicated by the steep negative slope of the I_D-V_{DS} curves at high V_{DS} range. On the other hand, even though its current density is more than twice that of the planar, the MMC device exhibited less negative slope of the I_D-V_{DS} curves suggesting weaker self-heating.

The insets in Figures 3(b) and 4(b) show T_A dependence of I_D at different values of V_{DS} ranging from 12 to 15 V of the planar and MMC devices, respectively. This suitably narrow range of V_{DS} was chosen to keep the R_{TH} essentially constant as mentioned above. The insets reveal well-behaved linear variation of I_D with T_A for different values of V_{DS}, verifying the I_D-T_A linear relationship assumption rendering the method of Menozzi *et al.* applicable.[17] Following step (2) in Fig. 2, from the best fit lines, the values of the slope h for each V_{DS} were then determined. Figures 3(b) and 4(b) show the plot of the reciprocal of h plotted as a function of V_{DS} for the planar and MMC devices, respectively. Following step (3), the extracted values of R_{TH}, which is the slope of the best fit line for the planar and MMC devices, are 419 K/W and 136 K/W, respectively. These values compare well with those given in Ref. 17. The R_{TH} of the MMC device is only ~32% that of the planar device, although its current density is more than twice that of the planar device. Multiplied to their respective effective gate widths, we obtained 42 K-mm/W and 4.8 K-mm/W values of R_{TH} for the planar and MMC devices, respectively. Incidentally, to further confirm its repeatability, we perform the same R_{TH} extraction method on another MMC device having a W_{top} of ~70 nm and 250 periods of mesa-trench structures within the gate electrode width of 100 μm, giving an effective total gate width W_{total} of 17.5 μm, with all other dimensions (L_G, L_{GD}, and L_{GS}) equal to that of the earlier MMC device. We obtained an R_{TH} value of 272 K/W, which when multiplied to the effective gate width $W_{total} = 17.5$ μm, translates to 4.8 K-mm/W. Remarkably, this value is exactly equal to that of the earlier MMC device with W_{total} of 35 μm. The lowest reported thermal resistance value of AlGaN/GaN HEMTs to date is 4.1 K-mm/W achieved by fabricating the device on low thermal resistivity but highly expensive single-crystal diamond (111) substrates.[11] The value of R_{TH} for our MMC device compares well to this record value considering that our devices are fabricated on more thermally resistive but cheaper and technologically mature sapphire substrates.

It can be argued that the lower R_{TH} of the MMC device relative to that of the planar device is due to its slightly lower raw current and relatively wider access region. For a fairer comparison, we also fabricated an *equivalent* planar device having a $W_{total} = 40$ μm, which is almost equal to the W_{total} of the MMC device whose I_D-V_{DS}-T_A curves were shown in Fig. 4. For the *equivalent* planar device illustrated in Fig. 5(a), edges of the channel under the metal gate are etched so that a single channel island remains at the center having a total channel width W_{total} almost equal to that of the MMC device. Both the MMC and equivalent planar devices have L_G of 1 μm, L_{GD} of 10 μm and L_{GS} of 2 μm, and device width W of 200 μm. From Fig. 5(b), interestingly, even if it has a slightly larger W_{total}, the *equivalent* planar structure has only about 60% of the raw I_D of the MMC device. Nevertheless, the *equivalent* planar device exhibited steeper negative slope of the I_D-V_{DS} curves, suggesting more severe self-heating. Following the same R_{TH} extraction method, we obtained a value of 474 K/W for the *equivalent* planar device or 19 K-mm/W considering the effective width. These results support the earlier claim that the MMC device has significantly less thermal resistance than conventional devices with planar gate structures.

The reduced thermal resistance in MMC devices can be attributed to its unique structure under the metal gate. Relative to the conventional planar device, because of its higher impedance, the channel region of the MMC device

This article is copyrighted as indicated in the article. Reuse of AIP content is subject to the terms at: http://scitation.aip.org/termsconditions. Downloaded to IP: 133.87.166.132 On: Tue, 16 Dec 2014 06:13:52

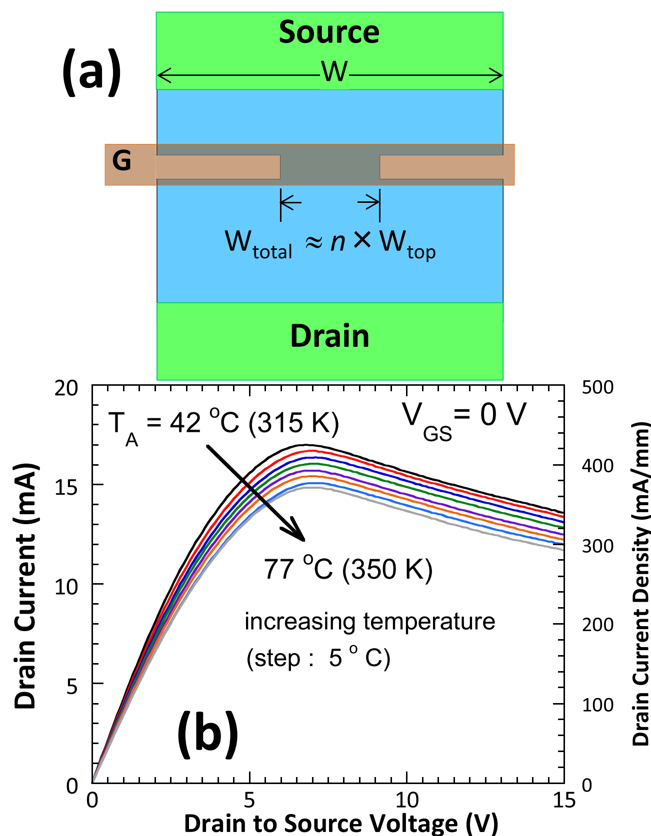

FIG. 5. (a) Schematic plan view of the *equivalent* planar device illustrating W_{total}. (b) T_A dependence of I_D-V_{DS} curves of the *equivalent* planar device with W_{total} of 40 μm.

dissipates a greater percentage of the total power dissipation P_D. Also, as schematically illustrated in Fig. 6, the proximity of the "cold" GaN regions below the trenches, which serve as the heat spreader, to the "hot" GaN regions below the current carrying mesa channel structures and to the "hotspots" localized at the G-D edge[4,10,26] gives high heat spreading ability to the MMC device. Particularly, the "hot" GaN regions are directly adjacent to "cold" GaN regions creating a large temperature gradient which drives heat to flow laterally. The heat can then be conducted towards the substrate or radiated to ambient. For the planar device, because of the absence of this mesa-trench structure, such lateral heat flow perpendicular to the direction of the current is substantially smaller. Moreover, the width of the "hot" mesa region (W_{top})

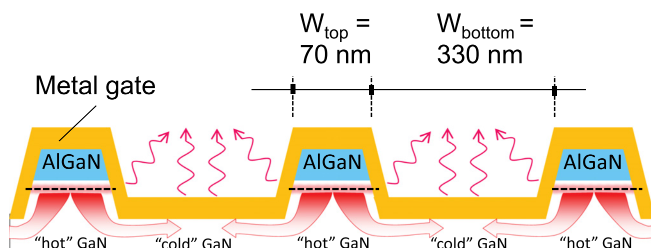

FIG. 6. Heat conduction away from the active mesa-channels schematic illustration (not drawn to scale). Regions of GaN buffer directly below the trenches are relatively cold compared to those regions directly below the active mesa-channels. The adjoining "cold" regions below the trenches can efficiently divert heat away from the mesa-channels and hotspots localized near the drain side of the gate edge. The heat is then radiated to ambient or conducted away towards the substrate.

is very small typically more than four times smaller than that of "cold" GaN region (W_{bottom}). This relative largeness of the heat spreading "cold" region, compared with the "hot" region, also plays a part in the high heat spreading ability of the MMC structure. These "cold" regions extend all the way down to the substrate, providing a parallel heat path through the substrate to ambient. In addition, the mesa side-walls and the "cold" GaN regions below the trenches facilitate heat radiation to ambient providing direct parallel thermal paths to ambient. Effectively, these parallel thermal resistances give the MMC device a substantially reduced thermal resistance compared to the conventional planar device. Our structure-based approach to thermal management is rather radical because it intends to spread the heat flow through the "cold" GaN regions which are several tens or hundreds of nanometer away from the source of heat. Conventional methods use heat spreaders which are few microns away from the heat source.[27] Moreover, because of the low thermal resistivity of GaN, it alleviates the effect of the high thermal resistivity of AlGaN barrier layer on the device thermal characteristics.[28] Our approach is also compatible and can be used in combination with the conventional techniques such as using highly thermally conductive substrates and employing heat spreading layers. Another important implication of our results is that it can pave the way for the serious consideration of lithium gallate (LGO), which has only a lattice-mismatch of 0.19% with GaN, as a substrate for fabricating low-defect GaN-based transistors.[29,30] As LGO is thermally resistive, it requires front side cooling scheme which the MMC structure can offer.

In summary, we have demonstrated dramatic reduction of thermal resistance in AlGaN/GaN Multi-Mesa-Channel (MMC) HEMTs on sapphire substrates. Compared with the conventional planar device grown on the same chip, the MMC HEMT exhibits much less negative slope of the I_D-V_{DS} curves at the saturation region, indicating excellent suppression of self-heating effect. Using a method proposed by Menozzi and co-workers, we have obtained a thermal resistance value of 4.8 K-mm/W. This value compares well to 4.1 K-mm/W, which is the thermal resistance of AlGaN/GaN HEMTs on expensive single crystal diamond substrates and is the lowest reported value in literature. These recent results strongly suggest that due its unique device structure, the MMC device can be a promising alternative for better thermal management of high-power AlGaN/GaN HEMTS.

[1]U. K. Mishra, L. Shen, T. E. Kazior, and Y. F. Wu, Proc. IEEE **96**, 287 (2008).
[2]G. D. Via, J. G. Felbinger, J. Blevins, K. Chabak, G. Jessen, J. Gillespie, R. Fitch, A. Crespo, K. Sutherlin, B. Poling, S. Tetlak, R. Gilbert, T. Cooper, R. Baranyai, J. W. Pomeroy, M. Kuball, J. J. Maurer, and A. Bar-Cohen, Phys. Status Solidi C **11**, 871 (2014).
[3]H. Morkoc, *Handbook of Nitride Semiconductors and Devices: GaN-Based Optical and Electronic Devices* (Wiley-VCH, 2008).
[4]M. Kuball, J. M. Hayes, M. J. Uren, T. Martin, J. C. H. Birbeck, R. S. Balmer, and B. T. Hughes, IEEE Electron Device Lett. **23**, 7 (2002).
[5]J. Kuzmik, P. Javorka, A. Alam, M. Marso, M. Heuken, and P. Kordos, IEEE Trans. Electron Devices **49**, 1496 (2002).
[6]J. Joh, J. A. del Alamo, U. Chowdhury, T. M. Chou, H. Q. Tserng, and J. L. Jimenez, IEEE Trans. Electron Devices **56**, 2895 (2009).
[7]R. J. Trew, D. S. Green, and J. B. Shealy, IEEE Microw. Mag. **10**, 116 (2009).
[8]W. L. Liu and A. A. Balandin, J. Appl. Phys. **97**, 073710 (2005).

This article is copyrighted as indicated in the article. Reuse of AIP content is subject to the terms at: http://scitation.aip.org/termsconditions. Downloaded to IP: 133.87.166.132 On: Tue, 16 Dec 2014 06:13:52

[9]R. Gaska, Q. Chen, J. Yang, A. Osinsky, M. A. Khan, and M. S. Shur, IEEE Electron Device Lett. **18**, 492 (1997).
[10]N. Killat, M. Montes, J. W. Pomeroy, T. Paskova, K. R. Evans, J. Leach, X. Li, U. Ozgur, H. Morkoc, K. D. Chabak, A. Crespo, J. K. Gillespie, R. Fitch, M. Kossler, D. E. Walker, M. Trejo, G. D. Via, J. D. Blevins, and M. Kuball, IEEE Electron Device Lett. **33**, 366 (2012).
[11]K. Hirama, Y. Taniyasu, and M. Kasu, Appl. Phys. Lett. **98**, 162112 (2011).
[12]G. J. Riedel, J. W. Pomeroy, K. P. Hilton, J. O. Maclean, D. J. Wallis, M. J. Uren, T. Martin, U. Forsberg, A. Lundskog, A. Kakanakova-Georgieva, G. Pozina, E. Janzen, R. Lossy, R. Pazirandeh, F. Brunner, J. Wurfl, and M. Kuball, IEEE Electron Device Lett. **30**, 103 (2009).
[13]N. Tanaka, H. Takita, Y. Sumida, and T. Suzuki, Phys. Status Solidi C **5**, 2972 (2008).
[14]Z. Yan, G. X. Liu, J. M. Khan, and A. A. Balandin, Nat. Commun. **3**, 827 (2012).
[15]J. Sun, H. Fatima, A. Koudymov, A. Chitnis, X. Hu, H. M. Wang, J. Zhang, G. Simin, J. Yang, and A. A. Khan, IEEE Electron Device Lett. **24**, 375 (2003).
[16]J. Das, H. Oprins, H. F. Ji, A. Sarua, W. Ruythooren, J. Derluyn, M. Kuball, M. Germain, and G. Borghs, IEEE Trans. Electron Devices **53**, 2696 (2006).
[17]R. Menozzi, G. A. Umana-Membreno, B. D. Nener, G. Parish, G. Sozzi, L. Faraone, and U. K. Mishra, IEEE Trans. Device Mater. Reliab. **8**, 255 (2008).
[18]K. Ohi and T. Hashizume, Jpn. J. Appl. Phys., Part 1 **48**, 081002 (2009).
[19]K. Ohi, J. T. Asubar, K. Nishiguchi, and T. Hashizume, IEEE Trans. Electron Devices **60**, 2997 (2013).
[20]J. T. Asubar, K. Ohi, K. Nishiguchi, and T. Hashizume, Phys. Status Solidi C **11**, 857 (2014).
[21]D. S. Lee, H. Wang, A. Hsu, M. Azize, O. Laboutin, Y. Cao, J. W. Johnson, E. Beam, A. Ketterson, M. L. Schuette, P. Saunier, and T. Palacios, IEEE Electron Device Lett. **34**, 969 (2013).
[22]G. S. Simin, M. Islam, M. Gaevski, J. Y. Deng, R. Gaska, and M. S. Shur, IEEE Electron Device Lett. **35**, 449 (2014).
[23]R. Menozzi and A. C. Kingswood, IEEE Trans. Device Mater. Reliab. **5**, 515 (2005).
[24]R. Gaska, A. Osinsky, J. W. Yang, and M. S. Shur, IEEE Electron Device Lett. **19**, 89 (1998).
[25]S. P. McAlister, J. A. Bardwell, S. Haffouz, and H. Tang, J. Vac. Sci. Technol. A **24**, 624 (2006).
[26]Y. Ohno, M. Akita, S. Kishimoto, K. Maezawa, and T. Mizutani, Phys. Status Solidi C **0**, 57 (2002).
[27]G. H. Jessen, J. K. Gillespie, G. D. Via, A. Crespo, D. Langley, J. Wasserbauer, F. Faili, D. Francis, D. Babic, F. Ejeckam, S. Guo, and I. Eliashevich, Tech. Dig. - Proc. IEEE Compd. Semicond. Integr. Circuit Symp. **2006**, 271.
[28]C. Hodges, J. A. Calvo, S. Stoffels, D. Marcon, and M. Kuball, Appl. Phys. Lett. **103**, 202108 (2013).
[29]R. Quay, *Gallium Nitride Electronics* (Springer-Verlag, 2008).
[30]A. Christensen, W. A. Doolittle, and S. Graham, IEEE Trans. Electron Devices **52**, 1683 (2005).

This article is copyrighted as indicated in the article. Reuse of AIP content is subject to the terms at: http://scitation.aip.org/termsconditions. Downloaded to IP: 133.87.166.132 On: Tue, 16 Dec 2014 06:13:52